Physics Letters B 837 (2023) 137641

Contents lists available at ScienceDirect

Physics Letters B

journal homepage: www.elsevier.com/locate/physletb

# Sequential fission and the influence of $^{208}$Pb closed shells on the dynamics of superheavy element synthesis reactions

D.Y. Jeung [a], D.J. Hinde [a,*], M. Dasgupta [a], C. Simenel [a,b], E.C. Simpson [a], K.J. Cook [a], H.M. Albers [c], J. Buete [a], I.P. Carter [a], Ch.E. Düllmann [c,d,e], J. Khuyagbaatar [c,d], B. Kindler [f], N. Lobanov [a], B. Lommel [f], C. Mokry [d,e], E. Prasad [a,1], J. Runke [d,e], C. Sengupta [a,2], J.F. Smith [a,3], P. Thörle-Pospiech [d,e], N. Trautmann [e], K. Vo-Phuoc [a], J. Walshe [a], E. Williams [a], A. Yakushev [c,d]

[a] *Department of Nuclear Physics and Accelerator Applications, Research School of Physics, Australian National University, Canberra, ACT 2601, Australia*
[b] *Department of Fundamental and Theoretical Physics, Research School of Physics, Australian National University, Canberra, ACT 2601, Australia*
[c] *SHE Chemistry Department, GSI Helmholtzzentrum für Schwerionenforschung, 64291 Darmstadt, Germany*
[d] *SHE Chemistry Section, Helmholtz Institute Mainz, 55099, Mainz, Germany*
[e] *Department of Chemistry - TRIGA Site, Johannes Gutenberg-Universität Mainz, 55099, Mainz, Germany*
[f] *Target Laboratory, GSI Helmholtzzentrum für Schwerionenforschung, 64291 Darmstadt, Germany*

A R T I C L E   I N F O

*Article history:*
Received 7 November 2022
Received in revised form 17 December 2022
Accepted 20 December 2022
Available online 22 December 2022
Editor: D.F. Geesaman

*Keywords:*
Quasifission
Sequential fission
Superheavy element synthesis reactions
Shell effects

A B S T R A C T

Measured binary quasifission mass spectra in reactions with actinide nuclides show a large peak in yield near the doubly-magic $^{208}$Pb. This has generally been attributed to the enhanced binding energy of $^{208}$Pb causing a valley in the potential energy surface, attracting quasifission trajectories. To investigate this interpretation, binary quasifission mass spectra and cross-sections have been measured at near-barrier energies for reactions of $^{50}$Ti with actinide nuclides from $^{238}$U to $^{249}$Cf. Cross-sections have also been deduced for sequential fission (a projectile-like nucleus and two fragments from fission of the complementary target-like nucleus). Binary cross-sections fall from ∼70% of calculated capture cross-sections for $^{238}$U to only ∼40% for $^{249}$Cf, with a compensating increase in sequential fission cross-sections. The data are consistent with the $^{208}$Pb peak originating largely from sequential fission of heavier fragments produced in more mass-asymmetric primary quasifission events. These are increasingly suppressed as the heavy quasifission fragment mass increases above $^{208}$Pb. The important role of sequential fission calls for re-interpretation of quasifission characteristics and dynamics in superheavy element synthesis reactions.



## 1. Introduction

The heaviest elements with significant natural abundance are Th and U (atomic numbers Z=90,92) with lifetimes $\sim 10^{10}$ years. Much shorter-lived isotopes of elements with Z up to 118 (oganesson) have been synthesised [1–6] by nuclear fusion of two lighter nuclei. An example is the "hot fusion" reaction of $^{48}$Ca with $^{248}$Cm, used to form element 116 (livermorium) [2]. This process can be thought of as analagous to merging charged droplets of liquid. Those elements with Z ≥104 are called superheavy elements (SHE). They only exist due to stabilization of the nucleus by quantum shell effects [7,8]. Their synthesis and nuclear decay characteristics challenge models of nuclear reactions and structure [9], whilst atom-by-atom investigations of chemical properties probe the limits of the periodic table [10–14].

To synthesise SHE by nuclear fusion, two conditions must be met. Firstly, the two nuclei must be brought into contact, by providing enough kinetic energy to overcome their mutual Coulomb repulsion. Secondly, the shape must evolve from the *elongated* contact configuration to the *compact* shape of the shell-stabilised superheavy compound nucleus (CN). This probability $P_{CN}$ is small [15–20] because after contact the effective poten-

* Corresponding author.
*E-mail addresses:* dongyun.jeung@anu.edu.au (D.Y. Jeung), david.hinde@anu.edu.au (D.J. Hinde).
[1] Present address: Department of Physics, School of Mathematical and Physical Sciences, Central University of Kerala, Kasaragod 671314, India.
[2] Present address: ACRF Image X Institute, University of Sydney, Central Clinical School, Sydney, Australia.
[3] Present address: Advanced Technology Institute, University of Surrey, Guildford, Surrey, GU2 7XH, United Kingdom.

https://doi.org/10.1016/j.physletb.2022.137641
0370-2693/

tial is generally repulsive [21]. This results in strong competition from fast non-equilibrium processes: deep inelastic scattering (with masses close to those of the projectile and target) and quasifission [22–24,19] (with masses evolving towards symmetry). These typically occur in $10^{-21}$ to $10^{-20}$s [24–32].

Measurements of binary quasifission mass distributions in heavy ion reactions with actinide nuclides (used to synthesise all elements with Z>113) show a strong peak in cross-section near $^{208}$Pb [15,28,33–38]. This has been associated with extra stability resulting from the 82 protons and 126 neutrons of $^{208}$Pb filling spherical quantum shells ($^{208}$Pb is a so-called "doubly-magic" nucleus). This increased binding energy results in a valley in the calculated (zero temperature) potential energy surface (PES), leading to scission [21]. The valley has been thought to attract or intercept [21,28,33,39,37] trajectories over the PES that might otherwise have led to formation of a compact superheavy nucleus. The consequence of this interpretation is *enhancement* of the quasifission yield near $^{208}$Pb, and reduction of the SHE cross section. Other shells have also been predicted to similarly affect quasifission [40,41].

There may be a problem with the accepted interpretation of the $^{208}$Pb peak. An early experimental study [42] of $^{48}$Ca, $^{50}$Ti + $^{238}$U reactions concluded that sequential fission plays an important role in binary quasifission mass distributions. Sequential fission is a well-established process [43,44,42,45–47] by which a heavy nucleus produced in an initial (primary) reaction subsequently decays by fission, resulting in a three-body [44,46], or four-body [45–47] outcome. The three-body process relevant here is sketched in Fig. 1(a). Fission barriers fall rapidly for nuclides heavier than $^{208}$Pb, so sequential fission would be expected to result in increasing suppression of binary quasifission events as the heavy fragment mass increases above $^{208}$Pb.

In contrast with the experimental conclusion, contemporaneous calculations [23], also for reactions with $^{238}$U, indicated that sequential fission, though present, might have only a relatively small effect. This disagreement could in principle result from experimental problems, or uncertainties in the parameters used in the calculations. The discrepancy has not subsequently been investigated experimentally, nor have further calculations been made (to our knowledge) of the impact of sequential fission on binary quasifission mass distributions, in particular for SHE synthesis reactions with heavier (more fissile) actinide nuclides.

As a result, the role of sequential fission has not been considered in later interpretation of the $^{208}$Pb peak [21,28,33,39,37]. The effect of sequential fission on evaluating total capture cross-sections was, however, recently discussed [48,49].

Support for the idea that the $^{208}$Pb shells drive the dynamics came from time-dependent Hartree-Fock calculations (e.g. Ref. [28]). These showed that in actinide reactions, the most likely heavy fragment mass in quasifission is close to $^{208}$Pb. However, the implicit assumption (seemingly reasonable) that the yield should peak at the most likely (calculated) mass [28] is not consistent with very recent experimental data for reactions of Cr with (non-fissile) Pt [31]. The measured mean mass-split agrees well with TDHF calculations made for these reactions. However, the experimental mass spectra were not peaked at the mean, rather were approximately triangular in shape, with the peak yield close to the entrance-channel mass. Thus support from microscopic theoretical calculations may be less decisive than believed previously.

To resolve the conflicting assumptions and interpretations of experiments and calculations, a model-independent experimental study is desirable. In this Letter we report on a purely experimental investigation of the origin of the $^{208}$Pb peak, for reactions with actinide nuclides from $^{238}$U to $^{249}$Cf. The aim was to determine whether the small yields of binary quasifission fragments heavier than $^{208}$Pb result mainly (i) from trajectories being *attracted* to the $^{208}$Pb valley in the PES, or (ii) from sequential fission of heavier (actinide) fragments produced in an initial (*primary*) quasifission event. This would result in a three-body outcome, leading to *suppression* of products heavier than $^{208}$Pb in measured binary quasifission mass spectra. Importantly, this scenario would result in reduced *total* experimental cross sections of binary quasifission.

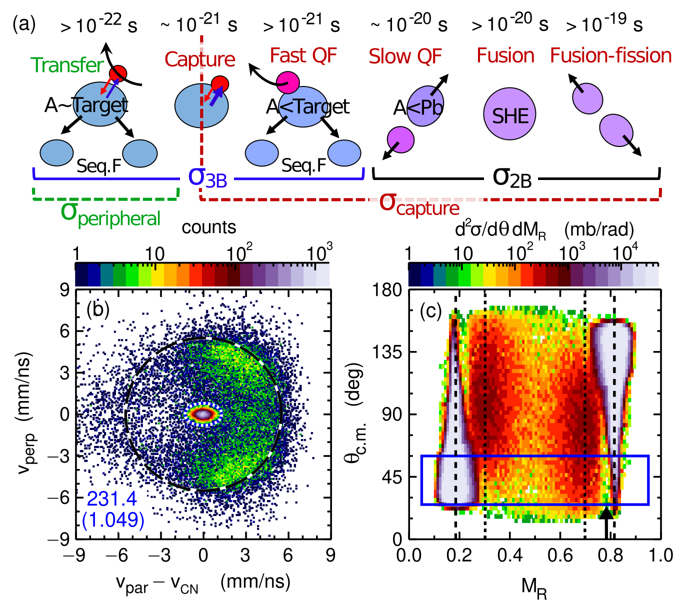


**Fig. 1.** (a) Two-body (2B) fission and quasifission (QF), and three-body (3B) sequential-fission (Seq.F) mechanisms. Characteristic times of the primary (binary) mechanism, heavy fragment masses A, and experimental and conceptual (perepheral and capture) cross-sections $\sigma$ are indicated. (b) Fission source velocity distribution [50,27,51,49] for all angles, for the $^{50}$Ti+$^{248}$Cm reaction at $E_{c.m.}$ = 231.4 MeV, 1.049 times the calculated [52] capture barrier energy $V_B$. The central blue-white dashed ellipse is used to select binary events. The large dashed circle, encompassing most events, shows the boundary for sequential fission when the projectile-like ejectile has the beam momentum. (c) Measured mass ratio vs. angle distribution (MAD) for binary events. The intensity scale (indicated above) is mb per radian per full (unity) $M_R$ range. The vertical dashed lines show the entrance-channel mass-ratio, dotted lines that for a $^{208}$Pb quasifission fragment. The arrow at $M_R$=0.79 indicates the region of missing events, attributed here to sequential fission. Mass-spectra in Fig. 3 are for 25° < $\theta_{c.m.}$ < 60° (blue rectangle).

The experiments included systematic measurements of binary quasifission mass distributions, and cross-sections of both binary and three-body (sequential) fission in reactions of $^{50}$Ti with the actinide nuclides $^{238}$U, $^{244}$Pu, $^{248}$Cm and $^{249}$Cf. The results from all observables consistently show that the $^{208}$Pb peak, a cornerstone of interpretation of the dynamics of SHE synthesis reactions, largely results from sequential fission of primary quasifission fragments heavier than $^{208}$Pb.

## 2. Experiment

The experiments were carried out at the ANU Heavy Ion Accelerator Facility. Pulsed beams [53,54] of $^{50}$Ti (pulses of width ≤ 1 ns separated by 106.7 ns) from the 14UD + Linac accelerators [55,56] bombarded targets of $^{238}$U, $^{244}$Pu, $^{248}$Cm and $^{249}$Cf at beam energies ranging from 0.98 to 1.15 of the capture barrier energies $V_B$ [52]. Targets comprised 30-160 μg/cm$^2$ of the actinide material, supported on 115-280 μg/cm$^2$ Al or Al/Ti backing foils [30]. Pairs of fission fragments, identified both by their individual and correlated velocities (corrected for fragment energy losses), were detected in coincidence using the CUBE detector system [50,57,27,30]. The position-sensitive multi-wire proportional counters gave continuous scattering angle coverage of 10° ≤ $\theta$ ≤ 80° on one side of the beam axis, and 55° ≤ $\theta$ ≤ 169° on the other, with typically 70° azimuthal angle coverage.

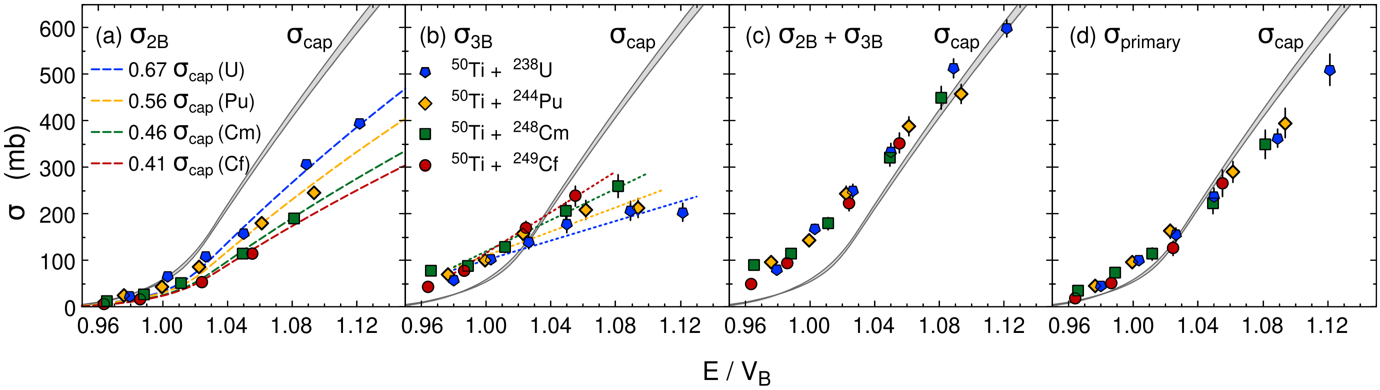


**Fig. 2.** Cross-sections as a function of E/$V_B$ for each reaction. The grey band encompasses the coupled-channels (CC) capture cross-sections $\sigma_{cap}$ for all reactions. (a) Measured binary quasifission cross-sections $\sigma_{2B}$ with dashed lines showing CC cross-sections for each reaction scaled by the indicated factor. (b) Extracted three-body sequential fission cross-sections $\sigma_{3B}$, with dotted lines representing linear fits to guide the eye. (c) Sum of $\sigma_{2B}$ and $\sigma_{3B}$. (d) Deduced primary quasifission cross-sections assuming the observed quasifission mass distributions extend linearly to the entrance channel masses (see text and Fig. 3).

Detected pairs of fission fragments can originate from a two-body final state (quasifission or fusion-fission), or from a three-body final state comprising a projectile-like nucleus and two fragments from the sequential fission of a target-like nucleus [49]. These mechanisms (illustrated in Fig. 1(a)) can be separated using the co-linearity of the two-body fragments in the centre-of-mass frame of the collision [49,50,27,51].

Components of the fission source velocity along the beam axis ($v_{par}$) and perpendicular to both the beam axis and the fission axis ($v_{perp}$) [50,27] can be determined experimentally. Optimum separation for these heavy projectiles is achieved by plotting ($v_{par} - v_{c.m.}$) as a function of $v_{perp}$ [50,58], as illustrated in Fig. 1(b) for 231.4 MeV $^{50}$Ti + $^{248}$Cm. The central peak corresponds to two-body events, whilst the surrounding “halo” comprises pairs of fission fragments from three-body events.

For the *two-body* events the fragment c.m. velocity vectors allow determination of the mass-ratio $M_R$ (the mass of one fragment divided by their sum) and $\theta_{c.m.}$, and thereby the generation of mass-angle distributions (MADs) [57,35,27]. With cross-section normalization using sub-barrier elastic scattering [19, 31], the MADs represent the double differential cross-section $d^2\sigma_{2B}/dM_R d\theta_{c.m.}$.

## 3. Results and analysis

An example of a binary quasifission MAD is shown in Fig. 1(c). This is for 231.4 MeV $^{50}$Ti + $^{248}$Cm, corresponding to an energy with respect to the calculated [52] capture barrier $V_B$ of E/$V_B$ = 1.049. The binary events were selected by the blue-white dashed elliptical gate in the centre of Fig. 1(b).

The MAD shows elastic, quasielastic and deep inelastic events close to the projectile-target mass-ratio (long dashed lines). Binary quasifission yields are peaked close to $^{208}$Pb (dotted lines), and extend to or beyond [31] mass-symmetry. Quasifission events are localised in angle, consistent with a short sticking time of ∼5 zs, typical for all these and similar [59,25,27,60,30] reactions. Significantly, there is a rapid drop in quasifission yield as $M_R$ values approach the projectile/target masses. This is seen best at angles where cross-sections of heavy target-like scattering recoils are weakest (indicated by the black arrow). The mass projection for the angular range $25° < \theta_{c.m.} < 60°$ (blue rectangle) is presented in Fig. 3(i), and will be discussed in Section 3.3.

The quantitative analysis of cross-sections that follows is applied to several independent experimental quantities: (i) the experimental cross-sections of two-body fission, which are compared to capture model calculations; (ii) ratios of three-body to two-body fission yields, allowing estimation of three-body cross-sections; and (iii) analysis of the binary quasifission mass spectra to estimate cross-sections lost to sequential fission.

### 3.1. Experimental binary quasifission cross sections

Total binary (2-body) quasifission cross-sections $\sigma_{2B}$ were obtained by extrapolating the measured angular distributions [Fig. 1(c)] to 0° and 180° by fitting with an empirical model of quasifission angular distributions [49]. In Fig. 2(a) the $\sigma_{2B}$ for all reactions are shown as a function of E/$V_B$. They are compared with capture cross-sections $\sigma_{cap}$ calculated using the coupled-channels code CCFULL [61] using a nuclear potential diffuseness of 0.65 fm. Couplings to static deformation of the targets, and vibrational states in the projectile and targets were included. The nuclear potential radii were then adjusted for each reaction to match [49] predicted mean capture barrier energies [52].

The calculations for all targets lie within the grey band. However, the experimental $\sigma_{2B}$ are different for each reaction, falling significantly with increasing target Z. The calculations match experiment only after scaling (dashed curves) by the indicated factors, which decrease monotonically from 0.67 for $^{238}$U to 0.41 for $^{249}$Cf.

This reduction with target Z is not consistent with trajectories being attracted to the $^{208}$Pb valley, since that mechanism should change the mass spectra, but *not* $\sigma_{2B}$. However, it could be consistent with an increasing fraction of sequential fission with higher target Z. This would be expected since the fraction of fissile actinide primary quasifission fragments produced in the primary quasifission process should be larger for higher target Z.

### 3.2. Sequential fission cross sections

The sequential fission yields themselves can give independent evidence for this interpretation. Fig. 1(b) shows that the two-body and three-body fission events are clearly separated using the deduced fission source velocity components. However, a potential problem is that correlation angles of sequential fission fragments can be widely spread due to the high momentum of the associated beam-like ejectile [49]. Only the large detector angular coverage in these measurements allowed this to be overcome. Selection of a specific limited range in lab. frame scattering and azimuthal angles for one sequential fission fragment ensured that the second fragment was detected with full geometrical efficiency in the other detector. For these measurements the selected scattering angles typically corresponded to mean centre-of-mass angles $\theta_{c.m.} \sim 105°$. Details of this procedure are described in Ref. [49].

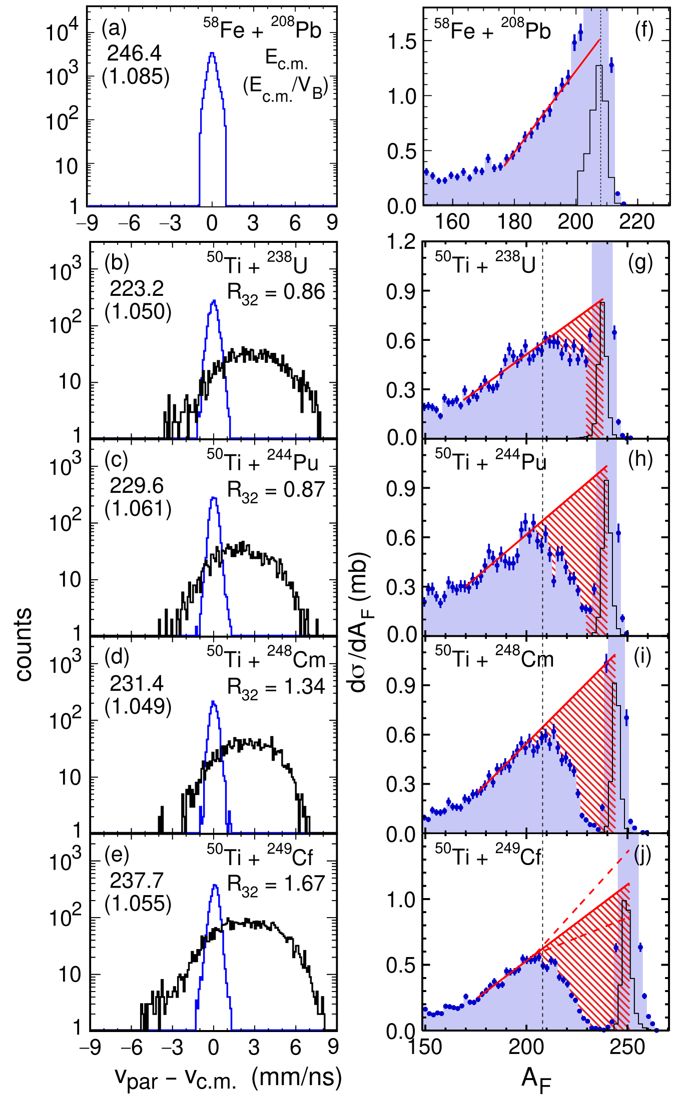


**Fig. 3.** (a)-(e): Measured spectra of $(v_{par} - v_{c.m.})$ for the angular selection where both fission fragments are detected with full efficiency (see text). Binary fission events (blue histogram) are selected by the blue-white dashed gate in Fig. 1(b), whilst three-body events (black) originate outside. The reactions, c.m. energies and $(E/V_B)$ are indicated. $R_{32}$ is the ratio of 3- to 2-body events. (f)-(j) show forward angle mass spectra $d\sigma_{2B}/dA_F$ for binary quasifission. The red line is a fit up to A∼200, extrapolated to the experimental (quasi)elastic peaks. These are shown by the scaled down histograms, having FWHM ∼4 u. The hatched area is assigned to sequential fission following capture; dashed lines in (j) correspond to ±20% uncertainty.

Resulting spectra of $(v_{par} - v_{c.m.})$ of binary quasifission events (blue) and three-body events (black) are shown in Fig. 3(a) to (e), at similar $E/V_B$ (given in brackets in each panel). The ratios $R_{32}$ of three-body to two-body fission events are also indicated. Note that $R_{32}$ nearly doubles between $^{238}$U and $^{249}$Cf.

To estimate the total three-body cross-section $\sigma_{3B}$, first the three-body differential cross-section was obtained by multiplying the 2-body differential cross-section by $R_{32}$. Since the angular distribution of the sequential fission fragments could not be determined experimentally, angular distributions with angular anisotropy A=1 and A=2 [62] were fitted to the three-body cross section obtained at $\theta_{c.m.} \sim 105°$, giving two $\sigma_{3B}$ values. The average was adopted for $\sigma_{3B}$, with the range giving the assigned uncertainty. This was always larger than that from counting statistics alone.

These $\sigma_{3B}$ are shown in Fig. 2(b). At $E/V_B \sim 1$ they are all similar, consistent with mainly non-capture origins such as sequential fission following multi-nucleon transfer (MNT), and some contribution from Coulomb excitation. At these lowest energies, where the fission cross-sections are small, there may also be some contamination in the sequential fission region of the source velocity spectra from random coincidences due to the high rate of scattered projectile and target nuclei. At the higher energies $\sigma_{3B}$ increases systematically with target Z. Indeed for the $^{248}$Cm and $^{249}$Cf reactions, the $\sigma_{3B}$ are larger than the $\sigma_{2B}$. This increase in $\sigma_{3B}$ with target Z is consistent with sequential fission being responsible for the observed reduction in $\sigma_{2B}$ with increasing target Z, clearly seen in Fig. 2(a).

The complementarity of $\sigma_{2B}$ and $\sigma_{3B}$ is demonstrated quantitatively in Fig. 2(c), where their sum is compared with $\sigma_{cap}$. All reactions show the same behaviour, demonstrating that the reduction in $\sigma_{2B}$ with increasing target Z is indeed associated with increasing sequential fission. The experimental $\sigma_{2B} + \sigma_{3B}$ are close to $\sigma_{cap}$ at the higher energies, but significantly higher at near-barrier energies. This excess is expected, since (as noted above) non-capture events will contribute increasingly to $\sigma_{3B}$ (as illustrated in Fig. 1(a)) when $E/V_B$ decreases [63,58].

Both $\sigma_{2B}$ and $\sigma_{3B}$ are consistent with a large cross-section of sequential fission following capture, increasing with target Z. It is concluded that capture must frequently result in sequential fission of heavy (actinide) nuclei produced in the *primary* mass-asymmetric quasifission decay, resulting in three-body events, as illustrated schematically in Fig. 1(a). This probability increases as the Z (and thus fissility) of the target nucleus increases, as would be expected.

### 3.3. *Binary quasifission mass spectra*

Are the measured mass spectra of the experimental binary quasifission events that survive sequential fission consistent with this picture?

For the binary events, multiplying $M_R$ by the compound nucleus mass gives the fragment mass number $A_F$ at scission (pre-scission evaporation should be negligible [26,64]). For $25° < \theta_{c.m.} < 60°$ (blue rectangle in Fig. 1(c)), the experimental spectra $d\sigma_{2B}/dA_F$ are shown in Fig. 3(g) to (j). The increase with target Z of the gap in yield between $^{208}$Pb (dotted line) and the target mass is clear. This is not because of experimental mass resolution, as the FWHM for quasielastic events was ∼4 u for all actinide targets.

Fig. 3(f) shows a contrasting mass spectrum observed for the $^{58}$Fe + $^{208}$Pb reaction, having similar charge product $Z_1Z_2$ = 2132 but negligible sequential fission. This shows an essentially linear increase in yield (associated with both quasifission and deep-inelastic products [19]) from A=175 to A=200 (red line in Fig. 3(f)). Significantly, similar behaviour was found for Cr+Pt reactions ($Z_1Z_2$ = 1872) [31], where the $^{208}$Pb closed shells cannot influence the quasifission characteristics.

With sequential fission already shown to be important, we now investigate the consequences if the primary quasifission mass distributions (before sequential fission) in the present *actinide* reactions were to also follow this trend.

Linear fits were made to the actinide mass spectra for $A_F$ = 170 to $A_F$ = 200, shown by red lines in Fig. 3(g) to (j)). These fits were extrapolated to the mass-centroids of the experimental quasielastic peaks (down-scaled histograms). If these extrapolations represent the true primary quasifission mass distributions, a significant fraction of capture events, increasing with target Z, is lost to sequential fission (red hatching). A ±20% uncertainty was assigned to the extrapolation (dashed lines in Fig. 3(j)). Extended to the full experimental angular range (the binary mass spectrum shape is essentially angle-independent), values of $\sigma_{primary}$ based on the linear extrapolation were obtained. These are compared in Fig. 2(d) for the different reactions, and with the capture calculations.

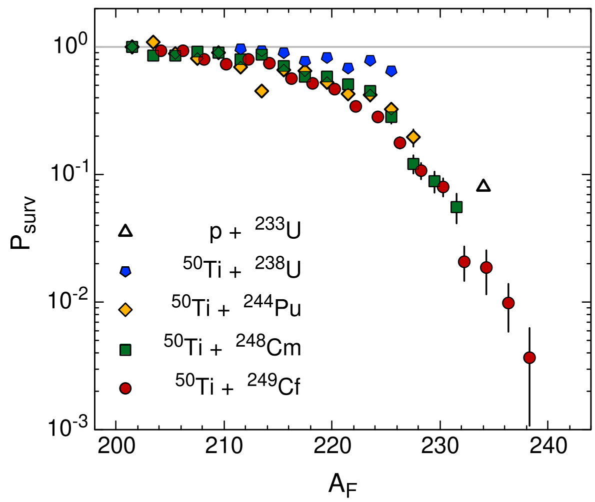


**Fig. 4.** Estimated sequential fission survival probabilities $P_{surv}$ as a function of the fragment mass number $A_F$. The open triangle is for p+$^{233}$U [67] for $E_x$ in the range 15-25 MeV. Uncertainties shown correspond only to statistical uncertainties in the measured $d\sigma/dA_F$.

### 3.4. Deduced primary quasifission cross-sections

The deduced $\sigma_{primary}$ for all targets show very similar values, and are close to the expectations for capture. This consistency supports the linear extrapolations of yield towards the entrance channel masses for the different reactions. More importantly, it demonstrates that the drop in the measured binary quasifission yield between the $^{208}$Pb peak and the target mass is the reason for the reduction in $\sigma_{2B}$ as the target Z increases (Fig. 2(a)). Furthermore, the $\sigma_{3B}$ results show conclusively that these missing cross-sections (corresponding to fissile actinide primary quasifission fragments) appear in the three-body sequential fission cross-sections. All results are thus consistent with the importance of sequential fission in these reactions.

A detailed comparison of the deduced $\sigma_{primary}$ with the calculated $\sigma_{cap}$ presented in Fig. 2(d) shows some disagreement. With increasing E/$V_B$, the $\sigma_{primary}$ are below the capture calculations, whilst at below-barrier energies they are consistently higher. This is likely to result from a combination of factors that can include: (i) uncertainties in the slope and form of the mass-yield extrapolation; (ii) the actual capture barriers being lower than calculated; (iii) missing channel couplings in the capture calculations; and (iv) expectations from experimental capture systematics [65] that capture cross-sections above-barrier should be below the calculated $\sigma_{cap}$. The latter reduction was suggested to be caused by kinetic energy loss *outside* the capture barrier, through the same mechanisms that result in deep inelastic scattering [49,65,66].

### 3.5. Sequential fission survival probabilities

A consistency check of the method used to extract $\sigma_{primary}$ can be made by evaluating the ratios of the experimental $d\sigma_{2B}/dA_F$ to the extrapolated primary fragment yields (red lines in Fig. 3(g) to (j)). This ratio represents the probability $P_{surv}(A_F)$ that heavy primary quasifission fragments with mass $A_F$ survive sequential fission.

$P_{surv}$ is plotted as a function of primary fragment mass $A_F$ in Fig. 4. $P_{surv}$ shows an increasingly steep fall with $A_F$. This might be expected from the decreasing liquid drop fission barriers resulting as $A_F$ (and thus the proton number $Z_F$) of the primary quasifission fragment increases.

The extracted $P_{surv}$ values are in reasonable agreement with the experimental [67] $P_{surv}$ for the p+$^{233}$U fusion reaction (with similar $A_F/Z_F$ to the systems measured here) of ~0.08 at excitation energies $E_x$ between 15 and 25 MeV.

In heavy ion reactions, the $P_{surv}$ are likely to be smaller because of expected higher angular momentum and $E_x$. Furthermore, shape polarization near scission due to the nearby complementary quasifission fragment has been postulated [68,69] to result in deformation of the heavy fragment outside its own fission barrier. This would result in a further decrease in $P_{surv}$.

The results in Fig. 4 suggest a (relatively weak) dependence of $P_{surv}$ on target mass for a given $A_F$. This result relies on the assumed linear extrapolation to estimate the primary quasifission $d\sigma_{primary}/dA_F$. Nevertheless, the result is reasonable, since more mass must necessarily be transferred from the higher mass target nuclides to reach a given $A_F$. This should be correlated with higher excitation energy [70], and thus greater fission probability.

### 3.6. A framework for binary quasifission mass distributions

The presence of significant sequential fission probabilities changes the variables controlling the *observed* binary quasifission mass distributions $d\sigma_{2B}/dA_F$. Including the effect of sequential fission, $d\sigma_{2B}/dA_F$ is determined by the product of the primary quasifission mass distribution $d\sigma_{primary}/dA_F$ and the sequential fission survival probability $P_{surv}(A_F)$:

$$d\sigma_{2B}/dA_F = [d\sigma_{primary}/dA_F].[P_{surv}(A_F)]. \quad (1)$$

$P_{surv}(A_F)$ should in fact have a stronger dependence on primary fragment charge than on mass. However, for a given reaction, the primary quasifission fragments are likely to have essentially the same Z/A as the compound nucleus, and thus effectively the function can be specified in terms of $A_F$.

It is clear from this equation that in the observed binary quasifission, a peak in both mass [28] and charge [38] near $^{208}$Pb would be expected to result from an increasing probability of sequential fission with primary fragment mass (and thus charge). It is well-known that the fission probability of excited nuclei near $^{208}$Pb is low, but increases rapidly with increasing charge and mass towards and beyond $^{238}$U.

It is also clear that the position of the peak in $A_F$ will depend on the shape of $d\sigma_{primary}/dA_F$ as well as on $P_{surv}(A_F)$. Even if $P_{surv}(A_F)$ were independent of reaction variables, the peak position could change for different entrance channels. This is because the shape of the $d\sigma_{primary}/dA_F$ distribution is expected to depend on the characteristics of the reaction, in particular the sticking time [25,31].

Key entrance channel variables affecting quasifission characteristics are known to be the effective entrance channel fissility [27] (depending largely on the charges of the two colliding nuclei), target deformation alignment [71,72,28] and E/$V_B$ [58]. Thus within the proposed explanation of the origin of the peak in binary quasifission yield near $^{208}$Pb, shifts in the position of the peak yield can be expected, and indeed have been observed [37], depending on the reaction.

## 4. Conclusions

In summary, all the cross-section measurements indicate that for reactions with heavy actinide nuclides, the peak in *binary* quasifission yields around $^{208}$Pb results largely from removal of heavier fragments produced in the *primary* quasifission process by their sequential fission, resulting in three-body outcomes. In previous investigations of quasifission in SHE synthesis reactions (e.g. Refs. [23,24,73,34,35,28,15,20]) these events have been removed by detector geometry and two-body event selection.

The current experimental results and analysis lead directly to the conclusion that the Pb peak seen in binary quasifission mass-spectra cannot now be taken as reliable evidence for the influence of Pb closed shells on quasifission dynamics. Further experimental investigation is required.

To determine the true effect of the Pb shells on the *primary* quasifission mass spectrum, measurements of all three fragments are called for. These data would also allow quantitative characterization of the sequential fission process itself for very heavy (actinide) primary quasifission fragments. This could potentially probe excitation energy division in the primary quasifission process, and the time scale of the sequential fission [46].

Major consequences of a significant role of sequential fission in superheavy element synthesis reactions include:

(i) The understanding of actinide reaction dynamics may need revision. The fall in measured *binary* quasifission yields above the $^{208}$Pb peak [23,34,36,15,30,20] for reactions with actinide nuclides provides separation from deep inelastic reaction outcomes. This suggests distinct mechanisms for these two processes. However, recent measurements where sequential fission is absent [74,19,31] found a continuous distribution of masses from deep inelastic products to quasifission. The present results suggest this may also be true in reactions with actinide nuclides.

(ii) Empirical values of $V_B$ extracted from $\sigma_{2B}$ may need revision in reactions where the sequential fission probability is high. The actual capture cross-section $\sigma_{cap} = \sigma_{2B}/(1-F_{3B})$, where $F_{3B}$ is the fraction of three-body events following capture. Significant changes in the 2-body mass spectrum are seen as $E_{c.m.}$ changes, suggesting that $F_{3B}$ (and thus the relationship between the measured $\sigma_{2B}$ and $\sigma_{cap}$) depends on $E_{c.m.}$.

(iii) Where sequential fission is very likely, binary quasifission events surviving sequential fission are likely to have excitation energies in the heavy partner significantly lower than the average of the primary quasifission events. This is because the fission probability will be lower at low excitation energy. This effect will potentially distort both the excitation energy division between fragments, and also the total kinetic energy spectra in binary quasifission events.

(iv) The empirical function [23] commonly used to describe the time-dependence of mass evolution in quasifission was derived from experimental binary quasifission mass and angle spectra in reactions with $^{238}$U. With a significant modulation of the mass spectrum by sequential fission, the *apparent* mean mass will be further from the entrance channel. This can be seen most clearly in Fig. 3(j). Thus the evolution of mass towards symmetry appears to be faster than in reality. Already experimental work where sequential fission should be less important [60] than in the current work, or completely absent [29], has found that mass evolution in quasifission indeed proceeds more slowly than the formula predicts. TDHF calculations for a wide range of systems also find mass evolution to be slower [75]. Thus the method of extraction of quasifission sticking times from mass spectra alone, making use of this standard mass evolution function, should be re-evaluated.

This work has shown that incorporating the effects of sequential fission is very important to allow correct interpretation of superheavy element synthesis reactions. The framework presented here can explain quantitatively the experimental results measured in this work, and appears consistent with prior experiments as well.

In general, clarification of mass and energy flows in actinide-based superheavy element synthesis reactions will allow better tests of models, leading to more accurate predictions of optimal reactions for the production of new superheavy elements and isotopes.

## Declaration of competing interest

The authors declare that they have no known competing financial interests or personal relationships that could have appeared to influence the work reported in this paper.

## Data availability

Data will be made available on request.

## Acknowledgements

The authors acknowledge the Australian Research Council for support through Discovery grants DP170102318, DP190101442, DP190100256, DP200100601. Financial support for accelerator operations was provided by the National Collaborative Research Infrastructure Strategy (NCRIS) through the Heavy Ion Accelerators (HIA) project. The authors acknowledge the support of the German Academic Exchange Service (DAAD) via funds of the German Federal Ministry of Education and Research (BMBF). The authors are grateful to W. Loveland for providing the $^{238}$U target.

## References

[1] S. Hofmann, G. Münzenberg, The discovery of the heaviest elements, Rev. Mod. Phys. 72 (2000) 733–767, https://doi.org/10.1103/RevModPhys.72.733.

[2] Yu.Ts. Oganessian, V.K. Utyonkov, Y.V. Lobanov, F.S. Abdullin, A.N. Polyakov, I.V. Shirokovsky, Y.S. Tsyganov, G.G. Gulbekian, S.L. Bogomolov, B.N. Gikal, A.N. Mezentsev, S. Iliev, V.G. Subbotin, A.M. Sukhov, A.A. Voinov, G.V. Buklanov, K. Subotic, V.I. Zagrebaev, M.G. Itkis, J.B. Patin, K.J. Moody, J.F. Wild, M.A. Stoyer, N.J. Stoyer, D.A. Shaughnessy, J.M. Kenneally, P.A. Wilk, R.W. Lougheed, R.I. Il'kaev, S.P. Vesnovskii, Measurements of cross sections and decay properties of the isotopes of elements 112, 114, and 116 produced in the fusion reactions $^{233,238}$U, $^{242}$Pu, and $^{248}$Cm + $^{48}$Ca, Phys. Rev. C 70 (2004) 064609, https://doi.org/10.1103/PhysRevC.70.064609.

[3] K. Morita, K. Morimoto, D. Kaji, T. Akiyama, S. ichi Goto, H. Haba, E. Ideguchi, R. Kanungo, K. Katori, H. Koura, H. Kudo, T. Ohnishi, A. Ozawa, T. Suda, K. Sueki, H. Xu, T. Yamaguchi, A. Yoneda, A. Yoshida, Y. Zhao, Experiment on the synthesis of element 113 in the reaction $^{209}$Bi($^{70}$Zn,n)$^{278}$113, J. Phys. Soc. Jpn. 73 (2004) 2593–2596, https://doi.org/10.1143/jpsj.73.2593.

[4] Yu.Ts. Oganessian, V.K. Utyonkov, Y.V. Lobanov, F.S. Abdullin, A.N. Polyakov, R.N. Sagaidak, I.V. Shirokovsky, Y.S. Tsyganov, A. Voinov, G. Gulbekian, S. Bogomolov, B. Gikal, A. Mezentsev, S. Iliev, V. Subbotin, A. Sukhov, K. Subotic, V. Zagrebaev, G. Vostokin, M. Itkis, K. Moody, J. Patin, D. Shaughnessy, M. Stoyer, N. Stoyer, P. Wilk, J. Kenneally, J. Landrum, J. Wild, R. Lougheed, Synthesis of the isotopes of elements 118 and 116 in the $^{249}$cf and $^{245}$cm+$^{48}$ca fusion reactions, Phys. Rev. C 74 (2006) 044602, https://doi.org/10.1103/PhysRevC.74.044602.

[5] Yu. Ts. Oganessian, F.S. Abdullin, P.D. Bailey, D.E. Benker, M.E. Bennett, S.N. Dmitriev, J.G. Ezold, J.H. Hamilton, R.A. Henderson, M.G. Itkis, Y.V. Lobanov, A.N. Mezentsev, K.J. Moody, S.L. Nelson, A.N. Polyakov, C.E. Porter, A.V. Ramayya, F.D. Riley, J.B. Roberto, M.A. Ryabinin, K.P. Rykaczewski, R.N. Sagaidak, D.A. Shaughnessy, I.V. Shirokovsky, M.A. Stoyer, V.G. Subbotin, R. Sudowe, A.M. Sukhov, Y.S. Tsyganov, V.K. Utyonkov, A.A. Voinov, G.K. Vostokin, P.A. Wilk, Synthesis of a new element with atomic number $z = 117$, Phys. Rev. Lett. 104 (2010) 142502, https://doi.org/10.1103/PhysRevLett.104.142502.

[6] Y.T. Oganessian, F.S. Abdullin, C. Alexander, J. Binder, R.A. Boll, S.N. Dmitriev, J. Ezold, K. Felker, J.M. Gostic, R.K. Grzywacz, J.H. Hamilton, R.A. Henderson, M.G. Itkis, K. Miernik, D. Miller, K.J. Moody, A.N. Polyakov, A.V. Ramayya, J.B. Roberto, M.A. Ryabinin, K.P. Rykaczewski, R.N. Sagaidak, D.A. Shaughnessy, I.V. Shirokovsky, M.V. Shumeiko, M.A. Stoyer, N.J. Stoyer, V.G. Subbotin, A.M. Sukhov, Y.S. Tsyganov, V.K. Utyonkov, A.A. Voinov, G.K. Vostokin, Production and decay of the heaviest nuclei $^{293,294}$117 and $^{294}$118, Phys. Rev. Lett. 109 (2012) 162501, https://doi.org/10.1103/PhysRevLett.109.162501.

[7] A. Sobiczewski, F. Gareev, B. Kalinkin, Closed shells for Z > 82 and N > 126 in a diffuse potential well, Phys. Lett. 22 (1966) 500–502, https://doi.org/10.1016/0031-9163(66)91243-1.

[8] V.M. Strutinsky, Shell effects in nuclear masses and deformation energies, Nucl. Phys. A 95 (1967) 420–442, https://doi.org/10.1016/0375-9474(67)90510-6.

[9] S. Giuliani, Z. Matheson, W. Nazarewicz, E. Olsen, P.-G. Reinhard, J. Sadhukhan, B. Schuetrumpf, N. Schunck, P. Schwerdtfeger, Colloquium: superheavy elements: oganesson and beyond, Rev. Mod. Phys. 91 (1) (2019), https://doi.org/10.1103/revmodphys.91.011001.

[10] P. Schwerdtfeger, O. Smits, P. Pyykkö, The periodic table and the physics that drives it, Nat. Rev. Chem. 4 (7) (2020) 359–380, https://doi.org/10.1038/s41570-020-0195-y.

[11] W. Nazarewicz, The limits of nuclear mass and charge, Nat. Phys. 14 (2018) 537–541, https://doi.org/10.1038/s41567-018-0163-3.

[12] V. Pershina, Relativistic effects on the electronic structure of the heaviest elements. Is the periodic table endless?, C. R., Chim. 23 (2020) 255–265, https://doi.org/10.5802/crchim.25.

[13] A. Yakushev, L. Lens, Ch.E. Düllmann, M. Block, H. Brand, T. Calverley, M. Dasgupta, A. Di Nitto, M. Götz, S. Götz, H. Haba, L. Harkness-Brennan, R.-D. Herzberg, F.P. Heßberger, D. Hinde, A. Hübner, E. Jäger, D. Judson, J. Khuyagbaatar, B. Kindler, Y. Komori, J. Konki, J. Kratz, J. Krier, N. Kurz, M. Laatiaoui, B. Lommel, C. Lorenz, M. Maiti, A. Mistry, C. Mokry, Y. Nagame, P. Papadakis, A. Såmark-Roth, D. Rudolph, J. Runke, L. Sarmiento, T. Sato, M. Schädel, P. Scharrer, B. Schausten, J. Steiner, P. Thörle-Pospiech, A. Toyoshima, N. Trautmann, J. Uusitalo, A. Ward, M. Wegrzecki, V. Yakusheva, First study on nihonium (nh, element 113) chemistry at TASCA, Front. Chem. 9 (2021) 753738, https://doi.org/10.3389/fchem.2021.753738.

[14] A. Yakushev, L. Lens, Ch.E. Düllmann, J. Khuyagbaatar, E. Jäger, J. Krier, J. Runke, H.M. Albers, M. Asai, M. Block, J. Despotopulos, A.D. Nitto, K. Eberhardt, U. Forsberg, P. Golubev, M. Götz, S. Götz, H. Haba, L. Harkness-Brennan, R.-D. Herzberg, F.P. Heßberger, D. Hinde, A. Hübner, D. Judson, B. Kindler, Y. Komori, J. Konki, J. Kratz, N. Kurz, M. Laatiaoui, S. Lahiri, B. Lommel, M. Maiti, A.K. Mistry, C. Mokry, K.J. Moody, Y. Nagame, J.P. Omtvedt, P. Papadakis, V. Pershina, D. Rudolph, L. Samiento, T. Sato, M. Schädel, P. Scharrer, B. Schausten, D.A. Shaughnessy, J. Steiner, P. Thörle-Pospiech, A. Toyoshima, N. Trautmann, K. Tsukada, J. Uusitalo, K.-O. Voss, A. Ward, M. Wegrzecki, N. Wiehl, E. Williams, V. Yakusheva, On the adsorption and reactivity of element 114, flerovium, Front. Chem. 10 (2022) 976635, https://doi.org/10.3389/fchem.2022.976635.

[15] E.M. Kozulin, G.N. Knyazheva, I.M. Itkis, M.G. Itkis, A.A. Bogachev, E.V. Chernysheva, L. Krupa, F. Hanappe, O. Dorvaux, L. Stuttgé, W.H. Trzaska, C. Schmitt, G. Chubarian, Fusion-fission and quasifission of superheavy systems with Z=110–116 formed in $^{48}$Ca-induced reactions, Phys. Rev. C 90 (2014) 054608, https://doi.org/10.1103/physrevc.90.054608.

[16] E.M. Kozulin, G.N. Knyazheva, K.V. Novikov, I.M. Itkis, M.G. Itkis, S.N. Dmitriev, Y.T. Oganessian, A.A. Bogachev, N.I. Kozulina, I. Harca, W.H. Trzaska, T.K. Ghosh, Fission and quasifission of composite systems with Z=108-120: transition from heavy-ion reactions involving S and Ca to Ti and Ni ions, Phys. Rev. C 94 (2016) 054613, https://doi.org/10.1103/physrevc.94.054613.

[17] E.M. Kozulin, G.N. Knyazheva, T.K. Ghosh, A. Sen, I.M. Itkis, M.G. Itkis, K.V. Novikov, I.N. Diatlov, I.V. Pchelintsev, C. Bhattacharya, S. Bhattacharya, K. Banerjee, E.O. Saveleva, I.V. Vorobiev, Fission and quasifission of the composite system Z=114 formed in heavy-ion reactions at energies near the Coulomb barrier, Phys. Rev. C 99 (2019) 014616, https://doi.org/10.1103/physrevc.99.014616.

[18] I.M. Itkis, E.M. Kozulin, M.G. Itkis, G.N. Knyazheva, A.A. Bogachev, E.V. Chernysheva, L. Krupa, Y.T. Oganessian, V.I. Zagrebaev, A.Y. Rusanov, F. Gönnenwein, O. Dorvaux, L. Stuttgé, F. Hanappe, E. Vardaci, E. de Goés Brennand, Fission and quasifission modes in heavy-ion-induced reactions leading to the formation of Hs*, Phys. Rev. C 83 (2011) 064613, https://doi.org/10.1103/PhysRevC.83.064613.

[19] K. Banerjee, D.J. Hinde, M. Dasgupta, E.C. Simpson, D.Y. Jeung, C. Simenel, B.M.A. Swinton-Bland, E. Williams, I.P. Carter, K.J. Cook, H.M. David, Ch.E. Düllmann, J. Khuyagbaatar, B. Kindler, B. Lommel, E. Prasad, C. Sengupta, J.F. Smith, K. Vo-Phuoc, J. Walshe, A. Yakushev, Mechanisms suppressing superheavy element yields in cold fusion reactions, Phys. Rev. Lett. 122 (2019) 232503, https://doi.org/10.1103/physrevlett.122.232503.

[20] K. Banerjee, D.J. Hinde, M. Dasgupta, J. Sadhukhan, E.C. Simpson, D.Y. Jeung, C. Simenel, B.M.A. Swinton-Bland, E. Williams, L.T. Bezzina, I.P. Carter, K.J. Cook, H.M. Albers, Ch.E. Düllmann, J. Khuyagbaatar, B. Kindler, B. Lommel, C. Mokry, E. Prasad, J. Runke, N. Schunck, C. Sengupta, J.F. Smith, P. Thorle-Pospiech, N. Trautmann, K. Vo-Phuoc, J. Walshe, A. Yakushev, Sensitive search for near-symmetric and super-asymmetric fusion-fission of the superheavy element flerovium (z=114), Phys. Lett. B 820 (2021) 136601, https://doi.org/10.1016/j.physletb.2021.136601, https://www.sciencedirect.com/science/article/pii/S0370269321005414.

[21] V. Zagrebaev, W. Greiner, Cross sections for the production of superheavy nuclei, Nucl. Phys. A 944 (2015) 257–307, https://doi.org/10.1016/j.nuclphysa.2015.02.010.

[22] B.B. Back, Complete fusion and quasifission in reactions between heavy ions, Phys. Rev. C 31 (1985) 2104, https://doi.org/10.1103/PhysRevC.31.2104.

[23] J. Tõke, B. Bock, G.X. Dai, A. Gobbi, S. Gralla, K.D. Hildenbrand, J. Kuzminski, W.F.J. Müller, A. Olmi, H. Stelzer, Quasi-fission – the mass-drift mode in heavy-ion reactions, Nucl. Phys. A 440 (1985) 327–365, https://doi.org/10.1016/0375-9474(85)90344-6.

[24] W.Q. Shen, J. Albinski, A. Gobbi, S. Gralla, K.D. Hildenbrand, N. Herrmann, J. Kuzminski, W.F.J. Müller, H. Stelzer, J. Tõke, B.B. Back, S. Bjørnholm, S.P. Sørensen, Fission and quasifission in U-induced reactions, Phys. Rev. C 36 (1987) 115–142, https://doi.org/10.1103/PhysRevC.36.115.

[25] R. du Rietz, D.J. Hinde, M. Dasgupta, R.G. Thomas, L.R. Gasques, M. Evers, N. Lobanov, A. Wakhle, Predominant time scales in fission processes in reactions of S, Ti and Ni with W: zeptosecond versus attosecond, Phys. Rev. Lett. 106 (2011) 052701, https://doi.org/10.1103/PhysRevLett.106.052701.

[26] D.J. Hinde, Neutron emission as a clock and thermometer to probe the dynamics of fusion-fission and quasi-fission, Nucl. Phys. A 553 (1993) 255c–270c, https://doi.org/10.1016/0375-9474(93)90627-a.

[27] R. du Rietz, E. Williams, D.J. Hinde, M. Dasgupta, M. Evers, C.J. Lin, D.H. Luong, C. Simenel, A. Wakhle, Mapping quasifission characteristics and timescales in heavy element formation reactions, Phys. Rev. C 88 (2013) 054618, https://doi.org/10.1103/PhysRevC.88.054618.

[28] A. Wakhle, C. Simenel, D.J. Hinde, M. Dasgupta, M. Evers, D.H. Luong, R. du Rietz, E. Williams, Interplay between quantum shells and orientation in quasifission, Phys. Rev. Lett. 113 (2014) 182502, https://doi.org/10.1103/physrevlett.113.182502.

[29] E. Prasad, D.J. Hinde, E. Williams, M. Dasgupta, I.P. Carter, K.J. Cook, D.Y. Jeung, D.H. Luong, C.S. Palshetkar, D.C. Rafferty, K. Ramachandran, C. Simenel, A. Wakhle, Fusion and quasifission studies for the $^{40}$Ca + $^{186}$W, $^{192}$Os reactions, Phys. Rev. C 96 (2017) 034608, https://doi.org/10.1103/physrevc.96.034608.

[30] H. Albers, J. Khuyagbaatar, D. Hinde, I. Carter, K. Cook, M. Dasgupta, Ch.E. Düllmann, K. Eberhardt, D. Jeung, S. Kalkal, B. Kindler, N. Lobanov, B. Lommel, C. Mokry, E. Prasad, D. Rafferty, J. Runke, K. Sekizawa, C. Sengupta, C. Simenel, E. Simpson, J. Smith, P. Thörle-Pospiech, N. Trautmann, K. Vo-Phuoc, J. Walshe, E. Williams, A. Yakushev, Zeptosecond contact times for element Z=120 synthesis, Phys. Lett. B 808 (2020) 135626, https://doi.org/10.1016/j.physletb.2020.135626.

[31] T. Tanaka, D.J. Hinde, M. Dasgupta, E. Williams, K. Vo-Phuoc, C. Simenel, E.C. Simpson, D.Y. Jeung, I.P. Carter, K.J. Cook, N.R. Lobanov, D.H. Luong, C. Palshetkar, D.C. Rafferty, K. Ramachandran, Mass equilibration and fluctuations in the angular momentum dependent dynamics of heavy element synthesis reactions, Phys. Rev. Lett. 127 (2021) 222501, https://doi.org/10.1103/PhysRevLett.127.222501.

[32] K. Hammerton, Z. Kohley, D.J. Hinde, M. Dasgupta, A. Wakhle, E. Williams, V.E. Oberacker, A.S. Umar, I.P. Carter, K.J. Cook, J. Greene, D.Y. Jeung, D.H. Luong, S.D. McNeil, C.S. Palshetkar, D.C. Rafferty, C. Simenel, K. Stiefel, Reduced quasifission competition in fusion reactions forming neutron-rich heavy elements, Phys. Rev. C 91 (2015) 041602, https://doi.org/10.1103/physrevc.91.041602.

[33] P. Gippner, K.D. Schilling, W. Seidel, F. Stary, E. Will, H. Sodan, S.M. Lukyanov, V.S. Salamatin, Y.E. Penionzhkevich, G.G. Chubarian, R. Schmidt, Shell effects in the evolution of the mass asymmetry in heavy-ion collisions leading to composite systems Z=108, Z. Phys. A 325 (1986) 335–346, https://doi.org/10.1007/bf01294618.

[34] M.G. Itkis, Y.T. Oganessian, V.I. Zagrebaev, Fission barriers of superheavy nuclei, Phys. Rev. C 65 (2002) 044602, https://doi.org/10.1103/physrevc.65.044602.

[35] D.J. Hinde, R. du Rietz, M. Dasgupta, R.G. Thomas, L.R. Gasques, Two distinct quasifission modes in the $^{32}$S +$^{232}$Th reaction, Phys. Rev. Lett. 101 (2008) 092701, https://doi.org/10.1103/PhysRevLett.101.092701.

[36] K. Nishio, S. Mitsuoka, I. Nishinaka, H. Makii, Y. Wakabayashi, H. Ikezoe, K. Hirose, T. Ohtsuki, Y. Aritomo, S. Hofmann, Fusion probabilities in the reactions $^{40,48}$Ca+$^{238}$U at energies around the Coulomb barrier, Phys. Rev. C 86 (2012) 034608, https://doi.org/10.1103/PhysRevC.86.034608.

[37] G.N. Knyazheva, I.M. Itkis, E.M. Kozulin, The time scale of quasifission process in reactions with heavy ions, J. Phys. Conf. Ser. 515 (2014) 012009, https://doi.org/10.1088/1742-6596/515/1/012009.

[38] M. Morjean, D.J. Hinde, C. Simenel, D.Y. Jeung, M. Airiau, K.J. Cook, M. Dasgupta, A. Drouart, D. Jacquet, S. Kalkal, C.S. Palshetkar, E. Prasad, D. Rafferty, E.C. Simpson, L. Tassan-Got, K. Vo-Phuoc, E. Williams, Evidence for the role of proton shell closure in quasifission reactions from X-ray fluorescence of mass-identified fragments, Phys. Rev. Lett. 119 (2017) 222502, https://doi.org/10.1103/physrevlett.119.222502.

[39] Y. Aritomo, Fusion hindrance and roles of shell effects in superheavy mass region, Nucl. Phys. A 780 (3) (2006) 222–246, https://doi.org/10.1016/j.nuclphysa.2006.09.018, http://www.sciencedirect.com/science/article/pii/S0375947406006348.

[40] K. Godbey, A.S. Umar, C. Simenel, Deformed shell effects in $^{48}$Ca$+^{249}$Bk quasifission fragments, Phys. Rev. C 100 (2019) 024610, https://doi.org/10.1103/PhysRevC.100.024610.

[41] C. Simenel, P. McGlynn, A.S. Umar, K. Godbey, Comparison of fission and quasi-fission modes, Phys. Lett. B 822 (2021) 136648, https://doi.org/10.1016/j.physletb.2021.136648.

[42] G. Guarino, A. Gobbi, K. Hildenbrand, W. Möller, A. Olmi, H. Sann, S. Bjørnholm, G. Rudolf, Mass drift in reactions between a heavy and a light nucleus, Nucl. Phys. A 424 (1984) 157–183, https://doi.org/10.1016/0375-9474(84)90133-7.

[43] J.V. Kratz, A.E. Norris, G.T. Seaborg, Mass-yield distributions in the reaction of $^{84}$Kr ions with $^{238}$U, Phys. Rev. Lett. 33 (1974) 502–505, https://doi.org/10.1103/PhysRevLett.33.502.

[44] J.V. Kratz, J.O. Liljenzin, A.E. Norris, G.T. Seaborg, Charge and mass distributions in the reaction of $^{40}$Ar ions with $^{238}$U, Phys. Rev. C 13 (1976) 2347–2365, https://doi.org/10.1103/physrevc.13.2347.

[45] P. Vater, E. Khan, R. Beckmann, P. Gottschalk, R. Brandt, Sequential fission studies in the interaction of 9.03 MeV/n 238u with natU using mica track detectors, Int. J. Radiat. Appl. Instrum., Part D, Nucl. Tracks Radiat. Meas. 11 (1–2) (1986) 5–16, https://doi.org/10.1016/1359-0189(86)90014-2.

[46] R. Charity, R. Freifelder, A. Gobbi, N. Hermann, K. Hildenbrand, F. Rami, H. Stelzer, J. Wessels, G. Casini, P. Maurenzig, A. Olmi, A. Stefanini, J. Galin, D.

Guerreau, U. Jahnke, A. Peghaire, J. Adloff, B. Bilwes, R. Bilwes, G. Rudolf, M. Petrovici, M. Gnirs, D. Pelte, Results on 2-body, 3-body, and 4-body events from the Mo-100+Mo-100 and sn-120+sn-120 collisions around e/a = 20 mev, Z. Phys. A, Hadrons Nucl. 341 (1) (1991) 53–73, https://doi.org/10.1007/BF01281274.

[47] A.A. Stefanini, G. Casini, P.R. Maurenzig, A. Olmi, R.J. Charity, R. Freifelder, A. Gobbi, N. Herrmann, K.D. Hildenbrand, M. Petrovici, F. Rami, H. Stelzer, J.P. Wessels, M. Gnirs, D. Pelte, J. Galin, D. Guerreau, U. Jahnke, A. Peghaire, J.C. Adloff, B. Bilwes, R. Bilwes, G. Rudolf, Analysis of the sequential fission observed in collisions of 100Mo + 100Mo and 120sn + 120sn around 20 a MeV, Z. Phys. A, Hadrons Nucl. 351 (2) (1995) 167–186, https://doi.org/10.1007/bf01289527.

[48] K.V. Novikov, E.M. Kozulin, G.N. Knyazheva, I.M. Itkis, M.G. Itkis, A.A. Bogachev, I.N. Diatlov, M. Cheralu, D. Kumar, N.I. Kozulina, A.N. Pan, I.V. Pchelintsev, I.V. Vorobiev, W.H. Trzaska, S. Heinz, H.M. Devaraja, B. Lommel, E. Vardaci, S. Spinosa, A. Di Nitto, A. Pulcini, S.V. Khlebnikov, P.P. Singh, R.N. Sahoo, B. Gall, Z. Asfari, C. Borcea, I. Harca, D.M. Filipescu, Investigation of fusion probabilities in the reactions with $^{52,54}$Cr,$^{64}$Ni, and $^{68}$Zn ions leading to the formation of $z = 120$ superheavy composite systems, Phys. Rev. C 102 (2020) 044605, https://doi.org/10.1103/PhysRevC.102.044605.

[49] D.Y. Jeung, D.J. Hinde, E. Williams, M. Dasgupta, E.C. Simpson, R. du Rietz, D.H. Luong, R. Rafiei, M. Evers, I.P. Carter, K. Ramachandran, C. Palshetkar, D.C. Rafferty, C. Simenel, A. Wakhle, Energy dissipation and suppression of capture cross sections in heavy ion reactions, Phys. Rev. C 103 (2021) 034603, https://doi.org/10.1103/PhysRevC.103.034603.

[50] D.J. Hinde, M. Dasgupta, J.R. Leigh, J.C. Mein, C.R. Morton, J.O. Newton, H. Timmers, Conclusive evidence for the influence of nuclear orientation on quasifission, Phys. Rev. C 53 (1996) 1290–1300, https://doi.org/10.1103/PhysRevC.53.1290.

[51] T. Banerjee, D.J. Hinde, D.Y. Jeung, K. Banerjee, M. Dasgupta, A.C. Berriman, L.T. Bezzina, H.M. Albers, Ch.E. Düllmann, J. Khuyagbaatar, B. Kindler, B. Lommel, E.C. Simpson, C. Sengupta, B.M.A. Swinton-Bland, T. Tanaka, A. Yakushev, K. Eberhardt, C. Mokry, J. Runke, P. Thörle-Pospiech, N. Trautmann, Systematic evidence for quasifission in $^{9}$Be -, $^{12}$C -, and $^{16}$O - induced reactions forming $^{258,260}$No, Phys. Rev. C 102 (2020) 024603, https://doi.org/10.1103/physrevc.102.024603.

[52] W.J. Świątecki, K. Siwek-Wilczyńska, J. Wilczyński, Fusion by diffusion. II. Synthesis of transfermium elements in cold fusion reactions, Phys. Rev. C 71 (2005) 014602, https://doi.org/10.1103/physrevc.71.014602.

[53] N.R. Lobanov, P. Linardakis, D. Tempra, Bunching and chopping for tandem accelerators. Part I: bunching, Nucl. Instrum. Methods Phys. Res., Sect. B, Beam Interact. Mater. Atoms 499 (2021) 133–141, https://doi.org/10.1016/j.nimb.2021.02.013, https://www.sciencedirect.com/science/article/pii/S0168583X21001361.

[54] N.R. Lobanov, P. Linardakis, D. Tempra, Bunching and chopping for tandem accelerators. Part II: chopping, Nucl. Instrum. Methods Phys. Res., Sect. B, Beam Interact. Mater. Atoms 499 (2021) 142–147, https://doi.org/10.1016/j.nimb.2021.02.014, https://www.sciencedirect.com/science/article/pii/S0168583X21001373.

[55] T. Ophel, J. Harrison, J. Newton, R. Spear, E. Titterton, D. Weisser, The 14ud pelletron accelerator at the Australian national university, Nucl. Instrum. Methods 122 (1974) 227–234, https://doi.org/10.1016/0029-554X(74)90485-6.

[56] T. Kibédi, D. Weisser, N. Lobanov, R. Turkentine, A. Muirhead, D. Anderson, The anu linac cryogenic system, in: Proceedings of the Seventh International Conference on Heavy Ion Accelerator Technology, Nucl. Instrum. Methods Phys. Res., Sect. A, Accel. Spectrom. Detect. Assoc. Equip. 382 (1) (1996) 167–171, https://doi.org/10.1016/S0168-9002(96)00455-X, https://www.sciencedirect.com/science/article/pii/S016890029600455X.

[57] R.G. Thomas, D.J. Hinde, D. Duniec, F. Zenke, M. Dasgupta, M.L. Brown, M. Evers, L.R. Gasques, M.D. Rodriguez, A. Diaz-Torres, Entrance channel dependence of quasifission in reactions forming $^{220}$Th, Phys. Rev. C 77 (2008) 034610, https://doi.org/10.1103/PhysRevC.77.034610.

[58] D.J. Hinde, D.Y. Jeung, E. Prasad, A. Wakhle, M. Dasgupta, M. Evers, D.H. Luong, R. du Rietz, C. Simenel, E.C. Simpson, E. Williams, Sub-barrier quasifission in heavy element formation reactions with deformed actinide target nuclei, Phys. Rev. C 97 (2018) 024616, https://doi.org/10.1103/physrevc.97.024616.

[59] D.J. Hinde, R. du Rietz, M. Dasgupta, R.G. Thomas, L.R. Gasques, Two distinct quasifission modes in the $^{32}$S + $^{232}$Th reaction, Phys. Rev. Lett. 101 (2008) 092701, https://doi.org/10.1103/PhysRevLett.101.092701.

[60] E. Prasad, A. Wakhle, D.J. Hinde, E. Williams, M. Dasgupta, M. Evers, D.H. Luong, G. Mohanto, C. Simenel, K. Vo-Phuoc, Exploring quasifission characteristics for $^{34}$S + $^{232}$Th forming $^{266}$Sg, Phys. Rev. C 93 (2016) 024607, https://doi.org/10.1103/PhysRevC.93.024607.

[61] K. Hagino, N. Rowley, A. Kruppa, A program for coupled-channel calculations with all order couplings for heavy-ion fusion reactions, Comput. Phys. Commun. 123 (1999) 143–152, https://doi.org/10.1016/s0010-4655(99)00243-x.

[62] B.B. Back, R.R. Betts, J.E. Gindler, B.D. Wilkins, S. Saini, M.B. Tsang, C.K. Gelbke, W.G. Lynch, M.A. McMahan, P.A. Baisden, Angular distributions in heavy-ion-induced fission, Phys. Rev. C 32 (1985) 195–213, https://doi.org/10.1103/PhysRevC.32.195.

[63] D. Hinde, J. Leigh, J. Bokhorst, J. Newton, R. Walsh, J. Boldeman, Mass-split dependence of the pre- and post-scission neutron multiplicities for fission of 251es, Nucl. Phys. A 472 (2) (1987) 318–332, https://doi.org/10.1016/0375-9474(87)90213-2.

[64] D.J. Hinde, D. Hilscher, H. Rossner, B. Gebauer, M. Lehmann, M. Wilpert, Neutron emission as a probe of fusion-fission and quasifission dynamics, Phys. Rev. C 45 (1992) 1229–1259, https://doi.org/10.1103/PhysRevC.45.1229.

[65] J.O. Newton, R.D. Butt, M. Dasgupta, D.J. Hinde, I.I. Gontchar, C.R. Morton, K. Hagino, Systematic failure of the Woods-Saxon nuclear potential to describe both fusion and elastic scattering: possible need for a new dynamical approach to fusion, Phys. Rev. C 70 (2004) 024605, https://doi.org/10.1103/PhysRevC.70.024605.

[66] M. Dasgupta, D.J. Hinde, A. Diaz-Torres, B. Bouriquet, C.I. Low, G.J. Milburn, J.O. Newton, Beyond the coherent coupled channels description of nuclear fusion, Phys. Rev. Lett. 99 (2007) 192701, https://doi.org/10.1103/PhysRevLett.99.192701.

[67] J.R. Boyce, T.D. Hayward, R. Bass, H.W. Newson, E.G. Bilpuch, F.O. Purser, H.W. Schmitt, Absolute cross sections for proton-induced fission of the uranium isotopes, Phys. Rev. C 10 (1974) 231–244, https://doi.org/10.1103/PhysRevC.10.231.

[68] K. Thomas, R. Davies, A.J. Sierk, Conditional saddle-point configurations, Phys. Rev. C 31 (1985) 915–922, https://doi.org/10.1103/PhysRevC.31.915.

[69] H. Deubler, K. Lekkas, P. Sperr, K. Dietrich, Kinetic energy and angular distributions of instantaneous fission fragments in a classical model, Z. Phys. A 284 (2) (1978) 237–244.

[70] J. Randrup, Theory of transfer-induced transport in nuclear collisions, Nucl. Phys. A 327 (2) (1979) 490–516, https://doi.org/10.1016/0375-9474(79)90271-9, https://www.sciencedirect.com/science/article/pii/0375947479902719.

[71] D.J. Hinde, A.C. Berriman, R.D. Butt, M. Dasgupta, C.R. Morton, A. Mukherjee, J.O. Newton, Influence of entrance channel properties on heavy-ion reaction dynamics, Eur. Phys. J. A 13 (2002) 149–154, https://doi.org/10.1140/epja1339-27.

[72] D.J. Hinde, R.G. Thomas, R. du Rietz, A. Diaz-Torres, M. Dasgupta, M.L. Brown, M. Evers, L.R. Gasques, R. Rafiei, M.D. Rodriguez, Disentangling effects of nuclear structure in heavy element formation, Phys. Rev. Lett. 100 (2008) 202701, https://doi.org/10.1103/PhysRevLett.100.202701.

[73] M.G. Itkis, Y.T. Oganessian, E.M. Kozulin, A.A. Bogatchev, I. Itkis, M. Jamdel, J. Kliman, G. Kniajeva, N.A. Kondratiev, J.V. Korzyukov, L. Krupa, I.V. Povrovski, V.A. Ponomarenko, E.V. Prokhorova, A.Y. Rusanov, V.M. Voskresenski, F. Hanappe, B. Benoit, T. Materna, N. Rowley, L. Stuttge, G. Giardina, K.J. Moody, Shell effects and the fission of superheavy nuclei at low excitation energies, in: Preprint E15-99-248, Joint Inst. of Nuclear Research, Dubna, 1999, pp. 1–10.

[74] E. Williams, K. Sekizawa, D.J. Hinde, C. Simenel, M. Dasgupta, I.P. Carter, K.J. Cook, D.Y. Jeung, S.D. McNeil, C.S. Palshetkar, D.C. Rafferty, K. Ramachandran, A. Wakhle, Exploring zeptosecond quantum equilibration dynamics: from deep-inelastic to fusion-fission outcomes in $^{58}$Ni + $^{60}$Ni reactions, Phys. Rev. Lett. 120 (2018) 022501, https://doi.org/10.1103/physrevlett.120.022501.

[75] C. Simenel, K. Godbey, A. Umar, Timescales of quantum equilibration, dissipation and fluctuation in nuclear collisions, Phys. Rev. Lett. 124 (2020) 212504, https://doi.org/10.1103/physrevlett.124.212504.